PHYSICAL REVIEW D

PARTICLES AND FIELDS

THIRD SERIES, VOLUME 27, NUMBER 11 1 JUNE 1983

Characteristics of neutral-current interactions induced by neutrinos

J. Marriner,* A. Barbaro-Galtieri, P. Bosetti,† G. Lynch, and M. L. Stevenson
Lawrence Berkeley Laboratory, University of California, Berkeley, California 94720

R. Benada,‡ U. Camerini, W. F. Fry, J. von Krogh,§ R. J. Loveless,
J. Mapp,** R. H. March, D. Minette,†† and D. D. Reeder
Department of Physics, University of Wisconsin, Madison, Wisconsin 53706
(Received 27 December 1982)

The ratio of neutral-current to charged-current interactions is measured to be 0.30 ± 0.03 for isoscalar targets, in good agreement with the results of previous experiments. Two independent methods are employed for isolating neutral-current events, one based on hadronic interactions, and the other on the momentum transverse to the hadron shower. The ratio of neutral-current interactions on neutrons to those on protons is measured to be 1.08 ± 0.19.

I. INTRODUCTION

The weak neutral current, a necessary component of the Weinberg-Salam theory of weak-electromagnetic interactions,[1] has been the subject of intense experimental investigation since its discovery in 1973.[2] In particular, the study of inclusive neutral-current scattering from isoscalar targets,[3–12] protons,[13–15] and neutrons[16–18] can illuminate the structure of this weak current. However, the reaction

$$\nu+N\rightarrow\nu+\text{hadrons} \tag{1}$$

is difficult to study because the outgoing neutrino, which typically carries half the interaction energy, cannot be detected, in contrast to the weak charged-current reaction

$$\nu(\bar{\nu})+N\rightarrow\mu^-(\mu^+)+\text{hadrons} \tag{2}$$

in which the muon is readily detected. Thus the understanding of weak neutral currents must come from the observation of only the hadronic final state. The heavy-liquid bubble chamber can provide information on the detailed structure of the inclusive hadronic final state which cannot be obtained with other techniques. Using the heavy-liquid bubble chamber all charged-hadron tracks are well measured, K_S^0 and Λ strange particles are observed, and some K_L^0 and neutrons are detected as neutral interactions. Typically greater than $\sim80\%$ of the hadronic energy is detected.

In this experiment we measure the inclusive neutral-current rate relative to the charged-current rate for neutrino interactions. By isolating a sample of neutral-current events the hadronic final state can be compared in detail to the hadrons in charged-current events, and to the hadronic system in other reactions. This comparison will be presented in another communication.[19] From the observed charge distribution of the events we extract the ratio of the cross section for the weak neutral current on neutrons to that on protons.

II. EXPERIMENTAL DETAILS

Details concerning the neutrino beam flux delivered to the 15-ft Fermilab bubble chamber by a horn-focused neutrino beam have been presented elsewhere.[20] The characteristics of the experiment relevant to this investigation are described below. The chamber was filled with a 34.5% molar mixture of neon in hydrogen. The density of the liquid was 0.28 g/cm^3, the radiation length was 111 cm, and the hadronic absorption length was measured to be 210 cm.

The bubble chamber was equipped with an external muon identifier (EMI),[21] which was immediately downstream of the bubble chamber and consisted of a layer of zinc absorber (3—5 absorption lengths) followed by a single plane of 24 multiwire proportional chambers (MWPC's). Each MWPC had a

delay-line readout of the wire (anode) plane and two cathode planes consisting of copper strips oriented at 45° and 90° with respect to the wire plane. A prompt time measurement was made from the ground circuit on the anode delay line. By reading out both ends of the delay lines constrained fits were made for most tracks which passed through the chambers. All tracks leaving the chamber with momentum greater than 3 GeV/c were extrapolated from the bubble chamber to the EMI. Most hadrons interacted in the zinc absorber and did not reach the MWPC while muons were unaffected except for multiple Coulomb scattering. Consequently, the distance between the extrapolated track and the nearest MWPC hit was normally large for hadrons and small for muons. A weight Φ derived from this distance was assigned to each track such that the average weight $\langle\Phi\rangle=1.0$ for muons and $\langle\Phi\rangle=0.0$ for hadrons. The details of this weighting procedure are described in the Appendix.

III. FILM ANALYSIS AND MEASUREMENT

The film was scanned for all interactions which were produced by an incident neutral particle. Events were required to have at least two outgoing tracks and greater than 3 GeV visible energy. Each track was visually identified to be (i) stopping in the chamber, (ii) an electron, (iii) an interacting or decaying track, or (iv) a track which leaves the chamber with no visible interactions. The muons, of course, belong to the last category. This classification is useful in the selection of neutral-current events, i.e., those containing no muon, and in eliminating background events due to ν_e and $\bar{\nu}_e$. From a rescan of a portion of the film we compute that the scan was $(90\pm5)\%$ efficient.

All tracks from the primary vertex were measured as were the downstream tracks which result from neutral-strange-particle decay, from neutral hadronic interactions, or from γ conversions into e^+e^- pairs. The events were constrained to be within a fiducial volume defined to be greater than 70 cm from the downstream wall and greater than 10 cm from any other wall of the chamber. This requirement defined a volume of 16.2 m^3 and, consequently, a target mass of 4.6 metric tons. Our complete sample consisted of 2690 interactions with visible energy $E_{\rm vis}$, greater than 5 GeV.

IV. NEUTRAL-CURRENT IDENTIFICATION

The sample of measured events can be divided into three categories by origin: (i) charged-current events (CC), (ii) neutral-current events (NC), and (iii) neutral-hadronic interactions initiated by neutrons or neutral kaons. The distinguishing feature of the charged-current interaction is the presence of an outgoing muon or electron which typically has a large fraction of the momentum of the incident neutrino. Since each of the four neutrinos $(\nu_\mu,\bar{\nu}_\mu,\nu_e,\bar{\nu}_e)$ produces its distinctive lepton (μ^-,μ^+,e^-,e^+), there is a unique signature for each type of charged-current event. Based on the scan for electron tracks we have identified the ν_e and $\bar{\nu}_e$ CC events with an estimated efficiency of 70%. By using the EMI we can define the muon-neutrino CC events without bias with respect to the charge of the muon. The events identified as ν_e or $\bar{\nu}_e$ CC interactions and $\bar{\nu}_\mu$ CC interactions for which a positive muon was identified[22] were removed from the sample.

Averaged over the observed neutrino spectrum, we calculate that 84% of the muons had a momentum greater than 3 GeV/c and were within the geometric acceptance of the EMI. The chambers were 95% efficient in recording muon tracks, thus approximately 80% of the muon tracks were correctly identified. However, because (1) the absorber was thin (i.e., 5% of the hadrons produce an acceptable EMI fit to the muon hypothesis) and (2) tracks unrelated to the neutrino interaction may intersect the chambers and accidentally match an extrapolated track, approximately 15% of the tracks interpreted by the EMI analysis as muons were misidentified (i.e., truly hadrons). One procedure to account for this misidentification would be to compute corrections for the loss of muons and the inclusion of the misidentified hadrons. However, this would require explicit knowledge of the distributions of hadrons which meet the muon selection criteria and will not be attempted. Instead, we shall determine the NC/CC rate in the sample by two indepen-

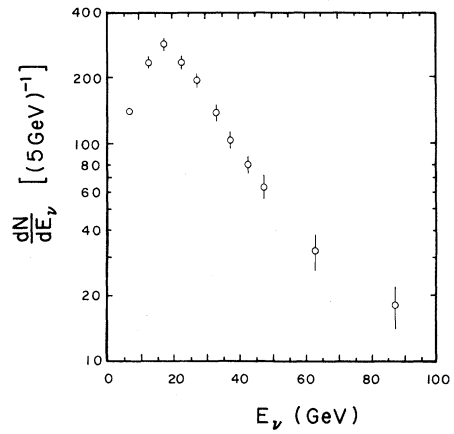

FIG. 1. Total neutrino-energy distribution for CC events corrected to include events with $p_\mu<3$ GeV by Monte Carlo calculation.

TABLE I. Interaction analysis.

	$E_{vis} > 5$ GeV	$E_{vis} > 10$ GeV
Total events	2690	2204
ν_μ CC ($p_\mu > 3$ GeV/c)	1681	1563
ν_μ CC ($p_\mu < 3$ GeV/c) (Monte Carlo)	267	193
Total ν_μ CC	1948	1756
Total ν_μ CC′ ($E_{had} > 5$ GeV, $n_{pr} > 2$)	1347±46	860±37
NC candidates (weighted)	780	428
Associated neutral-hadron events	138	41
Unassociated neutral-hadron events	117±21	32±11
ν_μ CC contamination of NC (Monte Carlo)	51	42
Residual $\nu_e, \bar{\nu}_e, \bar{\nu}_\mu$ events	39	35
Neutral-current events	435±43	278±31
NC/CC′	0.32±0.03	0.32±0.03
NC/CC′ (isoscalar)	0.30±0.03	0.30±0.03

dent methods. The first uses the probability that an event contains an EMI identified muon, while the second utilizes the characteristically large transverse momentum of the muon with respect to the hadrons.

A. Interaction method

For the first method we calculate the probability that each leaving track is a muon. From this probability we compute a weight (Φ) for each track such that the sum of the weights over a sample of tracks is equal to the total number of muons above 3 GeV/c in that sample (see the Appendix). We correct by a Monte Carlo simulation for the events whose muons have a momentum less than 3 GeV/c or which miss the EMI. In this Monte Carlo simulation we use the observed energy distributions of the neutrinos and parametrizations of the x and y scaling distributions obtained from other experiments.[23] The total number of CC events with E_{vis} greater than 5 (10) GeV so determined is 1948 (1756). The neutrino-energy distribution for these CC interactions, corrected for missing energy by balancing average transverse momentum, is shown in Fig. 1.

After the CC events with identifiable muons are removed, the NC events must be distinguished from incoming neutral-hadron interactions and from the CC events which have unidentified muons. The latter, expected to be about 20% of the total CC events, constitutes a significant background to the neutral-current signal.

To further reduce this background we require a NC candidate to be an event in which the negative track which has the largest component of momentum transverse to the ν direction ($p_\perp$) interacts in the visible volume of the bubble chamber. This requirement is motivated by the large transverse momentum imparted to the muon in the pointlike weak scattering. About 50% of the true NC events survive together with ~4% of the CC. To regain the total NC event sample we weight each NC candidate by the inverse of the interaction probability which has been measured as a function of momentum and visible length in the chamber. The numbers of

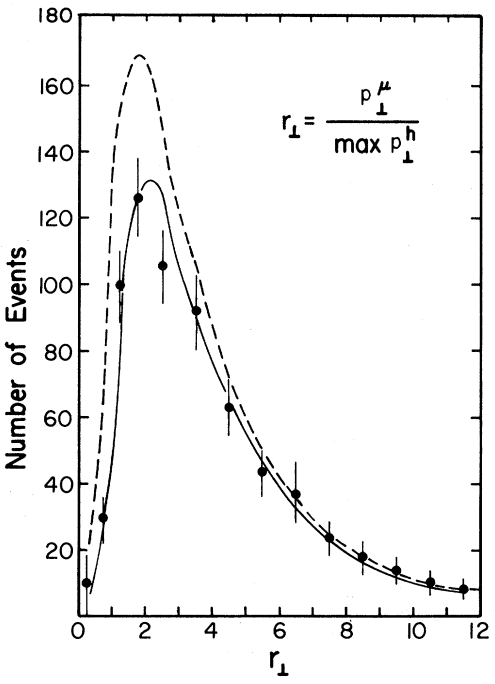

FIG. 2. The ratio of the muon $p_\perp$ to the maximum $p_\perp$ of the negative hadrons. The solid curve is the distribution derived from the Monte Carlo calculation for the observed data. The dashed curve (also obtained from Monte Carlo) shows the expected distribution for all CC events, including the low-energy muons.

events used in this calculation are given in Table I.

The CC events for which the muon does not have the largest $p_\perp$ are corrected by subtraction of the appropriate Monte Carlo calculated distribution. The magnitude of this correction is illustrated in Fig. 2, in which we plot the distribution of events in the variable $r_\perp$ which is the ratio of the $p_\perp$ of the muon to the largest value possessed by a negatively charged hadron. The events with $r_\perp < 1$ will satisfy the NC selection criterion. The experimental distribution observed in CC events with $p_\mu > 3$ GeV/c is shown in Fig. 2 together with the Monte Carlo calculation for these CC events and for the entire sample. For the former we observe 40 ± 12 events to be compared with the Monte Carlo calculation of 34. The calculated correction to the NC sample is 51 (42) events.

The remaining sample still contains a significant background of events which are neutral-hadron interactions. The extent of this background is determined by two independent methods.

(i) The association probability (b) is defined as the probability that a hadron event can be associated with its parent neutrino interaction. Associated events (i.e., those for which this connection is apparent) are eliminated. In Fig. 3 we plot the energy distribution for all events and for the associated events. Because the ν energy spectrum falls steeply below 5 GeV (Fig. 1) the events with $E_{\rm vis}$ in the range 1–3 GeV were assumed to be exclusively neutral-hadron events. From these the association probability was found to be $b=0.55\pm0.03$. The accidental association probability (f) was determined to be $f=0.041\pm0.006$ by comparing events (including wall events) from different frames. The determination of the number of hadron-induced events (N_h) can be accomplished using the relation

$$N_h = \frac{1-f}{b-f}N_A - \frac{f}{b-f}N_U \,, \tag{3}$$

where N_U (N_A) is the number of unassociated (associated) events. N_h is found to be 112 ± 35 events.

(ii) An alternative estimation of N_h can be made by assuming all charged and neutral tracks ($p > 5$ GeV/c) entering the bubble chamber are produced in upstream ν interactions. Using the CC sample H_c, the number of interacting charged tracks, and H_0, the number of interacting neutrals, were determined. The number of unassociated neutral-hadron events N_U can be found by scaling the number of unassociated charged-hadron events by H_0/H_c. From a scan of 1000 frames the rate of unassociated charged hadrons per frame was found to be $H_c=0.036\pm0.006$ (0.013 ± 0.004) for $E_{\rm vis}>5$ (10) GeV. The scaling factor H_0/H_c measured using the CC sample was 0.13 ± 0.05 (0.10 ± 0.07). Finally, we estimate $N_h=123\pm63$ (34 ± 26) events.

From these two independent results we calculate 117 ± 21 (32 ± 11) hadron events to be in the NC sample. Subtraction of N_h and the undetected events due to ν_e, $\bar{\nu}_e$, and $\bar{\nu}_\mu$ yields the final number of 435 (278) NC events in the sample. In order to compare to the CC events restrictions identical to those imposed on the NC sample must be made. The charged-current sample requiring ≥ 3 prongs and $E_{\rm had} > 5$ GeV (10 GeV) is denoted the CC′ sample. The ratio NC/CC′ is measured to be 0.32 ± 0.03 (0.32 ± 0.03). Table I contains the numbers used in this calculation.

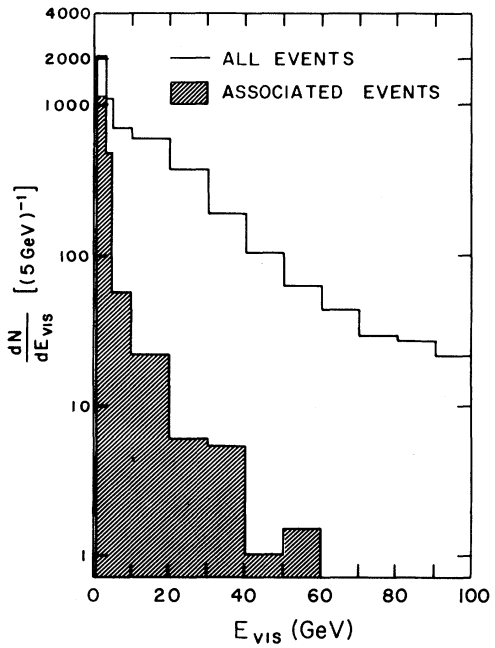

FIG. 3. The $E_{\rm vis}$ distribution for all events and for the subset of associated events (shaded). These associated events are typically neutral-hadron interactions with lower energy than the incident neutrinos.

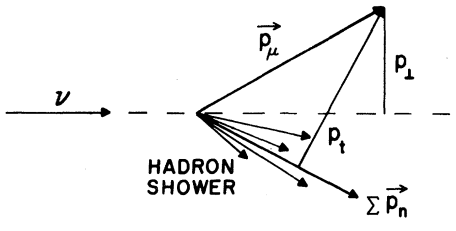

FIG. 4. A typical neutrino CC event defining $p_\perp$, momentum transverse to the neutrino direction, and p_t, momentum transverse to the vector sum of observed hadron tracks (both charged and neutral).

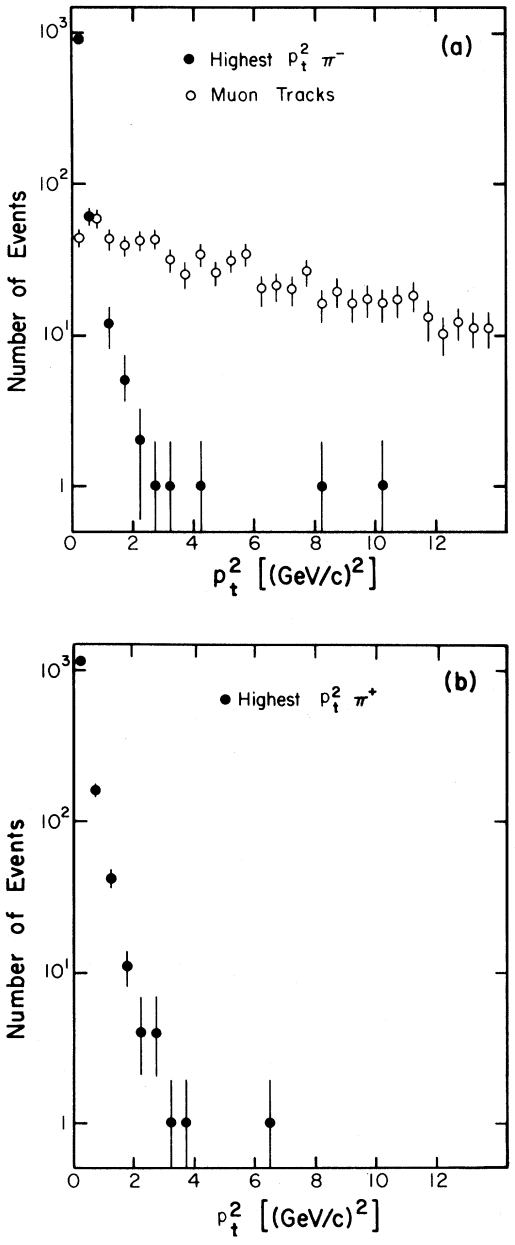

FIG. 5. (a) Distribution in p_t^2 for muons identified by the EMI. For CC events with such a muon the highest-p_t^2 negative track (other than the μ) is also shown. (b) The highest-p_t^2 positive track for CC events which have an identified μ^-.

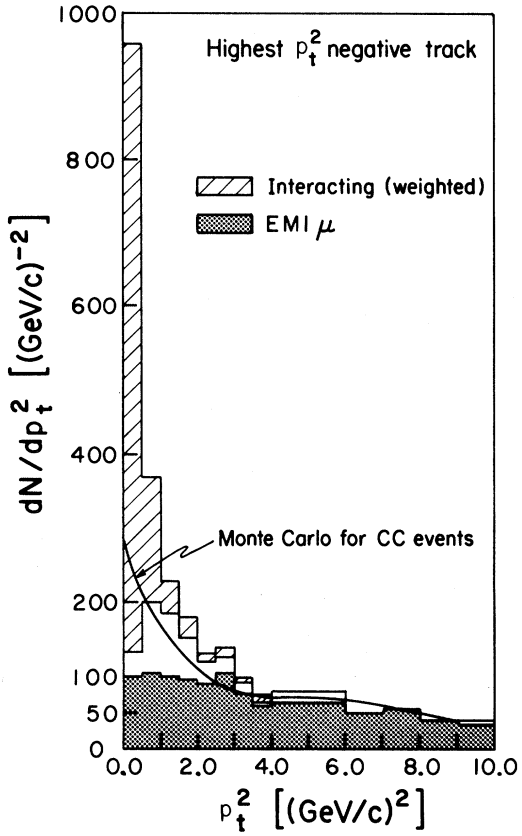

FIG. 6. The distribution of p_t^2 for the largest-p_t negatively charged track in each event which has $E_{\text{had}} > 5$ GeV. Tracks in the shaded area have been identified as μ^- by the EMI. The cross-hatched area represents the largest-p_t negative tracks which have interacted; each such track is weighted by the interaction probability. The solid curve represents the distribution of μ^- tracks for all CC events with $E_{\text{vis}} > 5$ GeV obtained from the Monte Carlo calculation.

B. Transverse-momentum method

The second method of muon identification exploits the fact that the distribution of the transverse momentum of one hadron calculated with respect to the vector sum of all hadron momenta is limited ($\langle p_t \rangle \sim 300$ MeV/c). In contrast, the muon has a large transverse momentum relative to the neutrino direction ($p_\perp$) and, by conservation of transverse momentum, has an even larger transverse momentum relative to the total hadron momentum (p_t). These definitions are shown in Fig. 4.

To illustrate the procedure we use the CC sample (i.e., events with an identified muon). The p_t^2 distribution for these muons is shown in Fig. 5(a). For each CC event the negative [positive] nonmuon track with the largest p_t^2 is plotted in Fig. 5(a) [5(b)]. The distributions are distinctly different for muons and hadrons. Thus events with a negative track having p_t^2 greater than 3.0 (GeV/c)^2 contain a muon and are charged-current events.

There remain a substantial number of CC events with $p_t^2 < 3.0$ (GeV/c)^2. This number can be estimated by normalizing a Monte Carlo simulation to the CC events with $p_t^2 > 3.0$ (GeV/c)^2. We estimate

TABLE II. Transverse-momentum analysis.

	$E_{vis} > 5$ GeV	$E_{vis} > 10$ GeV
Total events	2690	2204
Events with $n_{pr}=2$	220	152
Associated events	126	73
Net events	2344	1979
ν_μ CC ($p_\perp^2 > 3.0$ GeV/c^2)	1323	1237
Total events with $p_\perp^2 < 3.0$ GeV/c^2	1021	742
ν_μ CC ($p_\perp^2 < 3.0$ GeV/c^2) (Monte Carlo)	503±23	420±21
Unassociated neutral-hadron interactions	117±21	32±11
Residual $\nu_e, \bar{\nu}_e, \bar{\nu}_\mu$ interactions	34	31
NC events	367	259
Total CC ($n_{pr} > 3$)	1173±45	768±36
NC/CC	0.31±0.04	0.34±0.05
NC/CC (isoscalar)	0.29±0.04	0.32±0.05

535±23 CC events have $p_t^2 < 3.0$ for a total of 1173±45 CC events with $E_{vis} > 5$ GeV. This separation is graphically illustrated in Fig. 6 in which the distribution of p_t^2 is plotted for the entire event sample (excluding associated events and two-prong events). The number and disposition of these events are shown in Table II.

V. RESULTS

A. Neutral-current rate

As noted in Tables I and II the ratio of NC/CC′ was determined to be 0.32±0.03 for $E_{vis} > 5$ GeV. From the agreement between the interaction method and the transverse-momentum method we infer that there are no significant unknown systematic errors. Other experiments reporting a measurement of this ratio were performed using predominantly isoscalar targets (e.g., iron, marble, etc.) or in pure hydrogen. Our H_2-neon target contains 17% free protons and thus our result must be adjusted to correspond to an isoscalar target for comparisons to previous experimental data. The final isoscalar result becomes

$$\frac{\text{NC}}{\text{CC}'} = 0.30 \pm 0.03 \ . \tag{4}$$

This result is compared to previous measurements in Table III.

The distribution of visible hadronic energy (E_{had}) for the CC′ and NC events determined using the interaction method are shown in Fig. 7. A calculation of the characteristics of the neutral-current interaction as determined from measured quantities has been done by Kim *et al.*[24] based on a parametrization of the quark and gluon distribution functions suggested by Buras and Gaemers.[25] This calculation has been modified to include our energy spectrum and experimental restrictions, and the hadron energy distributions so determined are also shown in Fig. 7.

TABLE III. Recent NC results for isoscalar targets.

Experiment	Target	E_{had}cut (GeV)	$\frac{\text{NC}}{\text{CC}}$
HPWF (Ref. 5)	CH_2	4	0.30 ±0.04
CITF (Ref. 6)	Fe	12	0.28 ±0.03
BEBC (Ref. 7)	H_2-neon (74% molar)	15	0.32 ±0.03
CDHS (Ref. 8)	Fe	10	0.307±0.008
CHARM (Ref. 9)	Marble	2,10,17	0.320±0.010
CRS (Ref. 10)	H_2-neon (77% molar)	0.65	0.32 ±0.11
IMSTT (Ref. 11)	D_2	~5	0.30 ±0.03
ABBPPST (Ref. 12)	D_2	5	0.34 ±0.03
This experiment	H_2-neon (34% molar)	5	0.30 ±0.03

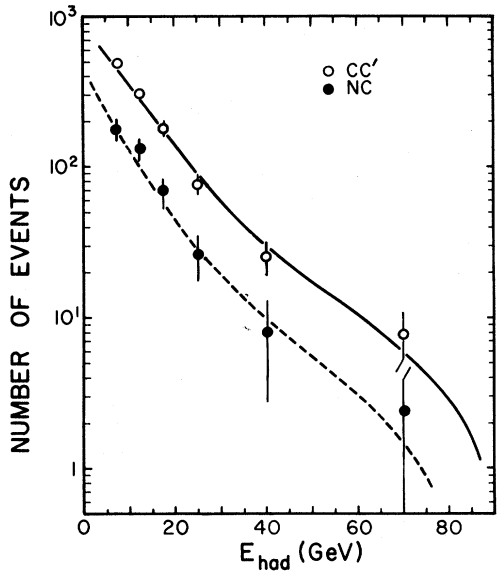

FIG. 7. Distribution of NC and CC' events weighted by the detection probability of each event as a function of the visible hadronic shower energy E_{had}. The solid curve (CC') and the dashed curve (NC) are the distributions calculated (Monte Carlo) according to the standard Weinberg-Salam model.

There is no significant variation of the ratio NC/CC' with hadronic energy, as is seen in Fig. 8.

B. Neutral-current interactions with protons and neutrons

Previous charged-current experiments have measured $\sigma_{\nu n}/\sigma_{\nu p}$ for ν_μ (Refs. 18 and 26–29) and $\bar{\nu}_\mu$ (Refs. 26, 28, 30, and 31). Neutral-current experiments reporting this ratio have studied ν_μ,[11,12] $\bar{\nu}_\mu$,[17]

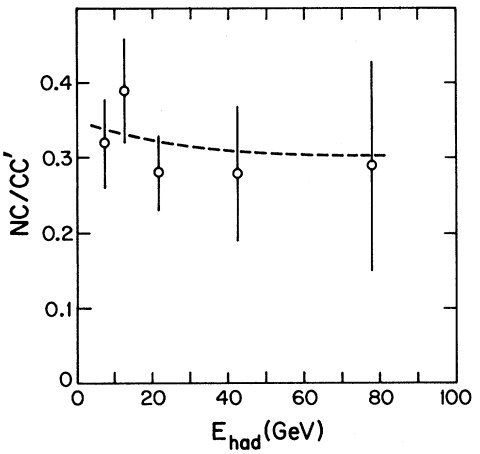

FIG. 8. The ratio NC/CC' as a function of hadronic energy E_{had}. The dashed curve is the predicted energy dependence of the ratio.

and low-energy ($E_\nu < 10$ GeV) ν_μ.[18] An early result from this experiment has been presented.[16]

The events with neutron targets can be separated from those with proton targets by means of the net charge of the event (i.e., the algebraic sum of track charges). In the absence of intranuclear scattering, neutron events would have net charge 0 and proton events net charge 1. In fact these charge distributions are considerably smeared. Most often the resultant net charge is positive but occasionally a negative net charge is observed in which a proton or nuclear fragment leaves a track too short to be visible. Other less frequent occurrences are charge-exchange scattering in the nucleus and mismeasurement of the charge of a track.

The cascade within the nucleus produces many low-energy nucleons and fragments. Exclusion of these from the computation of net charge reduces the spread of the distribution toward positive charge. We eliminate all tracks which stop within 2 cm of the vertex although the final results are not sensitive to small changes in this value of this minimum range.

Deviating slightly from the analysis performed earlier,[16] we adopt the simple model used by Efremenko *et al.*[31] in an analysis of $\bar{\nu}$ interactions in the same H_2-neon mixture. Let N_n, N_p, and N_H denote the true number of neutrino events occurring on neutron targets in neon, proton targets in neon, and hydrogen nuclei, respectively. We define W_i to be the probability that the visible charge will be shifted by i units from its true value. In addition we assume the ν cross section is identical for bound and free protons and that the W_i are independent of the charge of the target nucleus. With these assumptions we can write the following set of equations for the number of observed events with charge i, N_i^*:

$$N_1^* = W_1 N_n + W_0 N_p + W_0 N_H \,, \tag{5}$$

$$N_i^* = W_i N_n + W_{i-1} N_p \quad \text{for } -2 < i < 6,\ i \neq 1 \,, \tag{6}$$

$$\sum W_i = 1 \,. \tag{7}$$

Using the known nuclear composition of the H_2-neon mixture (the fraction of neutrons, bound protons, and hydrogen is 0.427, 0.418, and 0.155, respectively) we are left with 9 equations in 9 unknowns.

Rather than solve this poorly constrained system we can augment the number of equations by assuming the W_i are independent of whether a ν or $\bar{\nu}$ is incident on the nucleon. However, the analysis of the resultant system of 18 equations in 10 unknowns indicates that this assumption must be rejected. The

W_i depend significantly on the hadronic energy E_{had} which is distributed differently for ν and $\bar{\nu}$ (i.e., different scaling y distributions). However, because the hadronic energy distributions of neutrino-induced CC and NC events are more similar, this difficulty is not as serious for a simultaneous fit to these combined data.

The result of the combined NC-CC fit is that the ratio of neutron events to proton events ρ becomes

$$\rho_{CC}=1.78\pm0.40\ , \tag{8}$$

$$\rho_{NC}=0.94\pm0.22\ , \tag{9}$$

with $\chi^2/DF=1.1$

These are compared to previously reported measurements in Table IV. The value expected for ρ_{CC} on the basis of the quark-proton model is slightly less than 2.0. If the value of ρ_{CC} is fixed at the weighted average 1.95 (see Table IV) and the W_i and ρ_{NC} are determined from the 18 equations, the result is

$$\rho_{NC}=1.08\pm0.19,\ \ \chi^2/DF=0.9\ . \tag{10}$$

VI. SUMMARY AND CONCLUSIONS

In an exposure of the 15-ft bubble chamber to a horn-focused beam of neutrinos produced by a 300-GeV proton beam we have determined the ratio of neutral-current inclusive interactions to those of the charged current to be 0.30 ± 0.03. Also, by examining the net charge distribution of the events, we have determined the ratio of the neutral-current cross section on neutrons to that on protons to be 1.08 ± 0.19. Both results are in excellent agreement with the standard model of the unified weak and electromagnetic interactions proposed by Weinberg and Salam.[1]

ACKNOWLEDGMENTS

We acknowledge the effort and support of our colleagues from the University of Hawaii and CERN throughout the data run, particularly for the long effort necessary to build and maintain the EMI system. We also thank the 15-ft bubble-chamber crews and the measuring staffs of our respective institutions for an outstanding job well done. This work was supported in part by the U.S. Department of Energy.

APPENDIX

The EMI used in this experiment was composed of 25 proportional wire chambers each 1 m square located behind and outside the vacuum vessel of the chamber. Metallic zinc was placed between the coils such that about four absorption lengths were provided external to the chamber liquid. Details of the installation and performance have been published elsewhere.[21]

TABLE IV. $\sigma_{\nu n}/\sigma_{\nu p}$ ratios for CC and NC interactions.

Experiment	Target	$\frac{\sigma_{\nu n}}{\sigma_{\nu p}}$	$\frac{\sigma_{\bar{\nu} n}}{\sigma_{\bar{\nu} p}}$
	CC interactions		
CRS (Ref. 18)	H_2-neon (77% molar)	1.80±0.19	
IMSTT (Ref. 26)	D_2	2.03±0.28	0.51±0.16
BEBC-TST (Ref. 27)	H_2-neon (75% molar)	1.98±0.19	
ABPPST (Ref. 28)	D_2	2.22±0.28	0.51±0.03
BNL (Ref. 29)	D_2	1.95±0.10	
Gargamelle (Ref. 30)	Propane-heavy freon		0.46±0.10
FIIM (Ref. 31)	H_2-neon (34% molar)		0.45±0.08
This experiment	H_2-neon (34% molar)	1.78±0.40	
Weighted average		1.95±0.07	0.50±0.03
	NC interactions		
FIIM (Ref. 17)	H_2-neon (78% molar)		0.64±0.18
CRS (Ref. 18)	H_2-neon (77% molar)	1.07±0.24	
IMSTT (Ref. 11)	D_2	1.01±0.14	
ABBPPST (Ref. 12)	D_2	1.08±0.16	
This experiment	H_2-neon (34% molar)	1.08±0.19	(ρ_{CC} fixed at 1.95)
Weighted average		1.05±0.09	

For each track which passes through the EMI a confidence level c_μ for the muon hypothesis and a confidence level c_h for the hadron hypothesis are defined. c_μ is derived from the probability that a true muon would have a poorer match between the extrapolated position and the position measured in the proportional chamber. c_h is derived from the probability that a true hadron would have a better match.

Explicitly these confidence levels are defined to be

$$c_\mu=[(1-\epsilon)e^{(-\chi^2/2)}+\epsilon]e^{(-\pi\sigma_x\sigma_y\rho\chi^2)}, \tag{A1}$$

$$1-c_h=(1-e^{-\lambda})e^{(-\pi\sigma_x\sigma_y\rho\chi^2)}+c_\mu e^{-\lambda}, \tag{A2}$$

where σ_x and σ_y are the predicted horizontal and vertical errors, χ^2 is the chi squared of the match between the extrapolated position and the measured position,

$$\chi^2=\left[\frac{\Delta x}{\sigma_x}\right]^2+\left[\frac{\Delta y}{\sigma_y}\right]^2, \tag{A3}$$

ρ is the density of background hits in the EMI chambers, ϵ is the proportional chamber inefficiency, and λ is the track length measured in absorption lengths.

In general we can consider

$$c_\mu=c_\mu(\chi^2,\alpha_i), \tag{A4}$$

$$c_h=c_h(\chi^2,\alpha_i), \tag{A5}$$

where the functional dependence on χ^2 is explicitly shown and α_i are the remaining variables. For fixed α_i, χ^2 can be eliminated and a single relation is obtained:

$$c_h=c_h(c_\mu,\alpha_i). \tag{A6}$$

[Of course, the specific functional form of Eq. (A6) is different from that in Eq. (A5).] This relationship defines a curve in the c_h,c_μ plane for fixed α. Such a curve is shown in Fig. 9. The negative of the slope of the curve we define as L:

$$L=-\left.\frac{\partial c_\mu}{\partial c_h}\right|_\alpha. \tag{A7}$$

This definition is useful because it represents the distribution in the variable c_h of a sample of true muons. That is,

$$\frac{dN_\mu}{dc_h}=\frac{\partial c_\mu}{\partial c_h}\frac{\partial N_\mu}{\partial c_\mu}. \tag{A8}$$

If we have properly defined c_μ, the distribution of a sample of true muons in c_μ will be uniform. Thus

$$\frac{dN_\mu}{dc_h}=|L|. \tag{A9}$$

Of course, $|L|$ depends on the parameters α_i. In Fig. 9 we show the variation in $|L|$ for several values of the chamber background ρ. The curves are typical of those for a muon of 5 GeV/c momentum.

In order to estimate the number of muons in a sample of tracks a function $G(c_\mu,\alpha)$ is defined such that G averaged over a sample of muons has a different value than when averaged over a sample of hadrons. Although such a function is $|L|$ itself, another function was chosen for this analysis:

$$G=\frac{|L|}{|L|+1}. \tag{A10}$$

This function has the property of being ~ 1 for

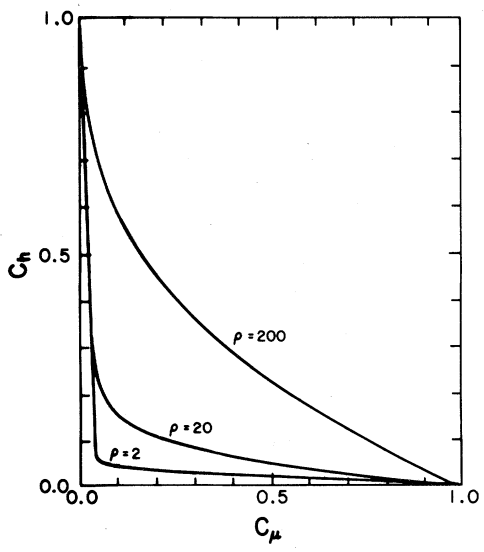

FIG. 9. A correlation plot of the confidence level of an EMI-measured track for the muon hypothesis c_μ and the hadron hypothesis c_h for several background hit densities ρ.

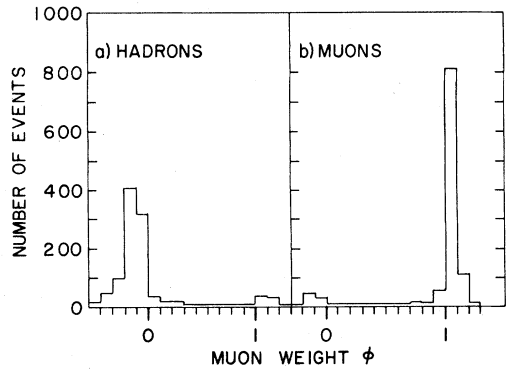

FIG. 10. The distribution in muon weight Φ for (a) a sample of true hadron tracks and (b) a sample of true muon tracks.

muons and ~ 0 for hadrons.

Using G we can estimate the number of muons in a sample of N tracks as

$$N_\mu = \sum_{i=1}^{N} \Phi_i = \sum \frac{G_i - \bar{G}_h}{\bar{G}_\mu - \bar{G}_h} \ . \tag{A11}$$

Equation (A11) defines Φ_i where $\bar{G}_h$ ($\bar{G}_\mu$) is the value of G averaged over a sample of true hadrons (muons). The variance of N_μ is then

$$\delta N_\mu \delta N_\mu = N_\mu \langle \Phi^2 \rangle \ , \tag{A12}$$

where $\langle \Phi^2 \rangle$ is the square of Φ_i averaged over the sample.

The method described above was tested by choosing an almost pure sample of muons or hadrons. The muon sample consisted of noninteracting tracks which traversed the entire chamber with momentum exceeding 10 GeV/c and within 2.5° of the ν beam direction. The sample of 450 tracks with these kinematic cuts was known to consist of (99.5±0.5)% muons. The estimate of the number of muons was 444±9 [(99±2)%]. The sample of hadrons was obtained using the CC events after removing the identified muon. The sample of 461 tracks contained (99±1)% hadrons. The estimate of the number of muons in this sample was 7±13 [(98±3)% hadrons]. A plot of the weight Φ is shown in Fig. 10 for both the muon and hadron samples.

---

*Present address: Fermilab, Batavia, Illinois 60510.
†Present address: Phys. Inst. der Tech. Hochschule, 5100 Aachen, Federal Republic of Germany.
‡Present address: 3126 Lakeland Ave., Madison, Wisconsin 53704.
§Present address: Inst. fur Hochenergiephysik, 6900 Heidelberg, Federal Republic of Germany.
**Present address: 1927 Commonwealth Ave., Madison, Wisconsin 53706.
††Present address: 2901 Elmside Ave., Houston, Texas 77042.

[1]S. Weinberg, Phys. Rev. Lett. 19, 1264 (1967); 27, 1688 (1972); Phys. Rev. D 5, 1412 (1972); A. Salam and J. C. Ward, Phys. Lett. 13, 168, (1964).

[2]For a recent comprehensive review of the experimental confirmation of the Weinberg-Salam model see J. E. Kim *et al.*, Rev. Mod. Phys. 53, 211 (1981). A prior review of the status of the Weinberg-Salam model is L. Sehgal, in *Neutrinos-78,* proceedings of the International Conference on Neutrino Physics and Astrophysics, edited by E. Fowler (Purdue University, West Lafayette, Indiana, 1978), p. 253, and a review of neutral-current experiments is given by K. Winter, in *Proceedings of the 1979 International Symposium on Lepton and Photon Interactions at High Energies, Fermilab,* edited by T. B. W. Kirk and H. D. I. Abarbanel (Fermilab, Batavia, Illinois, 1980), p. 253.

[3]G. Myatt, in *Proceedings of the Sixth International Symposium on Electron and Photon Interactions at High Energies, Bonn, 1973,* edited by H. Rollnik and W. Pfeil (North-Holland, Amsterdam, 1974), p. 389; F. J. Hasert *et al.*, Phys. Lett. 46B, 138 (1973); A. Benvenuti *et al.*, Phys. Rev. Lett. 32, 800 (1974); F. J. Hasert *et al.*, Nucl. Phys. B73, 1 (1974); B. Aubert *et al.*, Phys. Rev. Lett. 32, 1454 (1974); A. Benvenuti *et al.*, *ibid.* 32, 1457 (1974); P. Schreiner, in *Proceedings of the International Neutrino Conference, Aachen, West Germany, 1976,* edited by H. Faissner, H. Reithley, and P. Zerwas (Vieweg, Braunschweig, West Germany, 1977), p. 333; S. J. Barish *et al.*, Phys. Rev. Lett. 33, 448 (1974); B. C. Barish *et al.*, *ibid.* 34, 538 (1975); A. Benvenuti *et al.*, *ibid.* 37, 1039 (1976); D. Cline *et al.*, *ibid.* 37, 252 (1976); 37, 648 (1976); J. Blietschau *et al.*, Nucl. Phys. B114, 189 (1976).

[4]M. Holder *et al.*, Phys. Lett. 72B, 254 (1977).

[5]P. Wanderer *et al.*, Phys. Rev. D 17, 1679 (1978).

[6]F. S. Merritt *et al.*, Phys. Rev. D 17, 2199 (1978).

[7]H. Deden *et al.*, Nucl. Phys. B149, 1 (1979).

[8]C. Geweniger, in *Neutrino '79,* proceedings of the International Conference on Neutrinos, Weak Interactions, and Cosmology, Bergen, Norway, edited by A. Haatuft and C. Jarlskog (University of Bergen, Bergen, Norway), Vol. 2, p. 392.

[9]M. Jonker *et al.*, Phys. Lett. 99B, 265 (1981).

[10]C. Baltay *et al.*, Phys. Rev. Lett. 44, 916 (1980).

[11]T. Kafka *et al.*, Phys. Rev. Lett. 48, 910 (1982).

[12]P. H. A. van Dam, in *Proceedings of the International Conference Neutrino '82, Balatonfüred, Hungary, 1982,* edited by A. Frenkel and L. Jenik (Roland Eötvös University, Budapest, Hungary, 1982), Vol. II, p. 51.

[13]F. Harris, *et al.*, Phys. Rev. Lett. 39, 437 (1977).

[14]M. Derrick *et al.*, Phys. Rev. D 18, 7 (1978).

[15]J. Blietschau *et al.*, Phys. Lett. B88, 381 (1979).

[16]A preliminary result of this experiment has been available: J. Marriner, Lawrence Berkeley Laboratory Report No. LBL-6438, 1977 (unpublished).

[17]B. P. Roe, in *Neutrino '79* (Ref. 8), Vol. 2, 592.

[18]P. F. Jacques *et al.*, Phys. Rev. D 24, 1067 (1981).

[19]R. Benada *et al.* (unpublished).

[20]A. Malensek, Fermilab Report No. TM 717, 1977 (unpublished).

[21]R. Cence *et al.*, Nucl. Instrum. Methods 138, 245 (1970).

[22]A $\bar{\nu}_\mu$ CC event was required to have a positive leaving track with an EMI weight $\Phi_i > 0.5$. Since there were a considerable ($\sim 10\%$) number of hadrons misidentified as muons, we invoked the distribution in the scaling variable y for antineutrinos [$dN/dy \sim (1-y)^2$] and required the event to have $y < 0.5$. This selection directly removes $\sim 76\%$ of the $\bar{\nu}_\mu$ CC background.

[23]The Monte Carlo program is a slightly modified version of the program developed at Fermilab by W. G. Scott and collaborators. The scaling distributions were taken from S. M. Heagy *et al.*, Phys. Rev. D 23, 1045 (1981).
[24]J. E. Kim *et al.*, Rev. Mod. Phys. 53, 211 (1981).
[25]A. J. Buras and K. J. F. Gaemers, Phys. Lett. B71, 106 (1977).
[26]J. Hanlon *et al.*, Phys. Rev. Lett. 45, 1817 (1980).
[27]N. Armenise *et al.*, Phys. Lett. 102B, 374 (1981).
[28]D. Allasia *et al.*, Phys. Lett. 107B, 148 (1981).
[29]N. J. Baker *et al.*, Phys. Rev. D 25, 617 (1982).
[30]O. Erriquez *et al.*, Phys. Lett. 80B, 309 (1979).
[31]V. I. Efremenko *et al.*, Phys. Lett. 84B, 511 (1979).